Proceedings of the 2012 IFAC Workshop on Automatic Control in Offshore Oil and Gas Production, Norwegian University of Science and Technology, Trondheim, Norway, May 31 - June 1, 2012

Controllability analysis of severe slugging in well-pipeline-riser systems

Esmaeil Jahanshahi, Sigurd Skogestad [1]
and Anette H. Helgesen [2]

Department of Chemical Engineering, Norwegian University of Science and technology, Trondheim, NO-7491 (e-mail: skoge@ntnu.no).

Abstract: Active control of the production choke valve is the recommended solution to prevent severe slugging flow conditions at offshore oilfields. The focus of this work is to find the structure of a simple, yet robust anti-slug control system. In order to find suitable control variables for stabilization, a controllability analysis of the system with different available measurements or different combinations of them was performed. Moreover, for including robustness and performance requirements at the same time, the controllability analysis was extended to a mixed sensitivity $\mathcal{H}_\infty$ optimization problem. Two case studies were considered; first, the controllability analysis was performed on a pipeline-rise system using a 4-state model for comparing the results to the previous works. Next, using a 6-state model, the results were extended to a more general well-pipeline-riser system. The controllability results were in accordance with the practical experience in anti-slug control.

Keywords: Oil production, two-phase flow, severe slugging, controllability, $\mathcal{H}_\infty$ control.

1. INTRODUCTION

In an offshore oilfield, pipelines and risers transfer multiphase mixture of oil, gas and water from oil wells at the seabed to the surface processing facilities. Several kilometers of pipeline run on the seabed ending with risers to topside platforms (Godhavn et al. (2005)). Surface of the seabed is not even, and pipelines get the shape of the terrain irregularities. For example, where there is a hill or valley in the seabed, it makes a low-point in the pipeline. Liquid phases tend to accumulate at low-points, and it can block the gas flow. In low flow rate conditions, this blockage leads to formation of a slugging flow regime called terrain-slugging. If the low-point is located close to base of the riser and length of the slugs are comparable to the length of the riser, the flow condition is called "severe-slugging" or "riser-slugging". The severe-slugging is also characterized by large oscillatory variations in pressure and flow rate (Storkaas (2005), Storkaas and Skogestad (2007)).

The oscillatory flow condition in offshore multi-phase pipelines is undesirable and an effective solution is needed to suppress it. This behavior can be prevented by reducing the opening of the top-side choke valve. However, this conventional solution increases the back pressure of the valve and reduces the production rate from the oil wells. Other conventional solutions are costly design changes such as full separation or installing a large slug catcher after the production choke. Active control of the topside choke valve is the recommended solution to maintain a non-oscillatory flow regime together with the maximum possible production rate (Sivertsen et al. (2009)). The control system used for this purpose is called anti-slug control. This control system uses measurements such as pressure, flow rate or fluid density as the control variables and the topside choke valve is the main manipulated variable.

Anti-slug control systems in practice are not robust, and the slugging flow often occurs even in closed loop system because of large inflow disturbances or plant changes. Therefore, we need to find a robust control structure for anti-slug control systems which should be also very simple so that operators will use it easily. In this way, fundamental physical limitations of the system in terms of controllability must be taken into account. For example by manipulating a valve at an operating point with 90% opening, it is impossible to control its upstream pressure effectively.

Controllability of the system is evaluated by minimum achievable peaks of different closed-loop transfer functions. These bounds are independent from the controller design and they are physical property of the system. The control variables or a combinations of these resulting in smaller peaks are preferable. However, controllability analysis is a mathematical tool for linear systems. Knowing that nature of the sever-slugging and even the simplified model used in this work is highly nonlinear, controllability analysis only gives useful information about the necessary conditions and limitations.

For controllability analysis, a simplified dynamical model of the system is needed. A 4-state model was proposed by Jahanshahi and Skogestad (2011) and it is used as the first case study in this work. This model has been developed based on assumption of constant inlet mass flow rates.

⋆ Contribution to invited session on Production Stabilization
[1] Corresponding author
[2] Current affiliation of the third author is BP Norge AS.

The model is also extended to include an oil well as the inlet flow condition into the pipeline. The parameters in the simplified models were obtained by matching results to simulations using the more detailed OLGA model. In order to study riser-slugging dynamics, a stable dynamic is considered for the oil well and only pressure-driven nature of the flow is considered. The resulting model has six states, but a 5-state model has been used for the analysis. After linearizing the model, it was observed that two states regarding the mass of gas and liquid in the well have the same dynamic, resulting in one pole and one zero on the imaginary axis. To prevent numerical problems, a minimum-phase realization of the system with five states is used for the controllability analysis. In the control part, the $\mathcal{H}_\infty$ controller was designed based on the 5-state model, but it could be able to control the original 6-state model.

This paper is organized as the following. Simplified models for sever-slugging are introduced in Section 2. Afterwards, the theoretical background for the controllability analysis is given in Section 3. Controllability analysis results are presented in Section 4, and finally, the main conclusions and remarks will be summarized in Section 5.

2. SIMPLIFIED DYNAMICAL MODEL

2.1 Simple model for pipeline-riser system

Storkaas and Skogestad (2007) used a PDE-based *two fluid* model with 13 segments which resulted in a set of 50 ODEs. In their work, it was concluded that main dynamics of severe slugging in a pipeline-riser system can be captured by a simpler model. The model used for the pipeline-riser system in this work is a 4-state model.

$$\dot{m}_{G1} = w_{G,in} - w_{G,lp} \tag{1}$$
$$\dot{m}_{L1} = w_{L,in} - w_{L,lp} \tag{2}$$
$$\dot{m}_{G2} = w_{G,lp} - w_{G,out} \tag{3}$$
$$\dot{m}_{L2} = w_{L,lp} - w_{L,out} \tag{4}$$

Details about this model are given by Jahanshahi and Skogestad (2011). This model has been developed based on assumption of constant inflow rates $w_{G,in}$ and $w_{L,in}$. But, in more practical conditions liquid and gas come from a network of oil wells and the inflow rate is pressure-driven.

2.2 Pipeline-riser case study

The simplified 4-state model described by equations (1), (2), (3) and (4) is fitted to a test case in OLGA simulator using four tuning parameters. In the OLGA test case the pipeline diameter is 0.12 m and its length is 4300 m. Starting from the inlet, the first 2000 m of the pipeline is horizontal and the remaining 2300 m is inclined with a 1° angle. It causes 40.14 m descent and creates a low-point at the end of pipeline. Riser is a vertical 300 m pipe with the diameter of 0.1 m. The 100 m horizontal section with the same diameter as that of the riser connects the riser to the outlet choke valve. The feed into the system is nominally constant at 9 kg/s, with $w_L = 8.64\, kg/s$ (oil) and $w_G = 0.36\, kg/s$ (gas). The pressure after the choke valve (P_0) is nominally constant at 50.1 bar. This leaves the choke valve opening Z_2 as the only degree of freedom in the system.

2.3 Simple model for well-pipeline-riser system

In order to study effect of pressure-driven inflow, dynamics of an oil well is considered as the inlet boundary condition. Moreover, Skofteland et al. (2007) suggests that source of severe-slugging instability is at the bottom-hole of the well and pressure at this position is the best control variable. Considering the oil well dynamic is also helpful to study this possibility theoretically. Two state variables, for mass of gas and mass of liquid inside the oil well, are added to obtain the 6-state model:

$$\dot{m}_{G,w} = \alpha^m_{G,t} w_r - w_{G,in}, \tag{5}$$
$$\dot{m}_{L,w} = (1 - \alpha^m_{G,t}) w_r - w_{L,in}, \tag{6}$$

where $\alpha^m_{G,t}$ is the gas mass fractions at top of the well, given by equation (15). Production rate from the reservoir to the well can be described by the following linear relationship.

$$w_r = PI \max(0, P_r - P_{bh}), \tag{7}$$

where PI is productivity index of the well, P_r is the constant reservoir pressure and P_{bh} is the bottom-hole pressure of the well.

$$P_{bh} = P_{wh} + \rho_{mix} g L_w. \tag{8}$$

The other important variables in the well model consist of the average density of the two-phase mixture

$$\rho_{mix} = \frac{m_{G,w} + m_{L,w}}{V_w}, \tag{9}$$

density of the gas phase

$$\rho_{G,w} = \frac{m_{G,w}}{V_w - m_{L,w}/\rho_L}, \tag{10}$$

pressure at the well-head

$$P_{wh} = \frac{m_{G,w} R T_{wh}}{M_G (V_w - m_{L,w}/\rho_L)}, \tag{11}$$

and the average liquid volume fraction inside the well

$$\overline{\alpha}_{L,w} = \frac{m_{L,w}}{V_w \rho_L}. \tag{12}$$

In order to calculate the volume fractions at top of the well, the same assumptions as in the riser model by Jahanshahi and Skogestad (2011) are used.

$$\alpha_{L,t} = 2\overline{\alpha}_{L,w} - \alpha_{L,b} \tag{13}$$

In this case, because of high pressure at bottom-hole, fluid from the reservoir is saturated (Ahmed (2006)) and liquid volume fraction at the bottom is $\alpha_{L,b} = 1$. However, with a simple model it is not possible to predict the level of liquid in the well. Therefore, a tuning parameter $K_a \approx 1$ is added for the model fitting purpose.

$$\alpha_{L,t} = 2K_a \overline{\alpha}_{L,w} - 1 \tag{14}$$

The gas mass fraction at top of the well follows as

$$\alpha^m_{G,t} = \frac{(1 - \alpha_{L,t})\rho_{G,w}}{\alpha_{L,t}\rho_L + (1 - \alpha_{L,t})\rho_{G,w}}. \tag{15}$$

And the density of the mixture at top of the well is

$$\rho_{mix,t} = \alpha^m_{G,t}\rho_{G,w} + (1 - \alpha^m_{G,t})\rho_L. \tag{16}$$

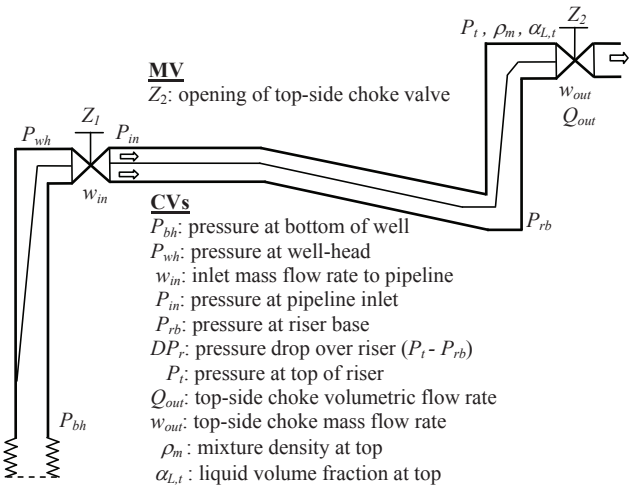

Fig. 1. Schematic presentation of candidate control variables and manipulated variable

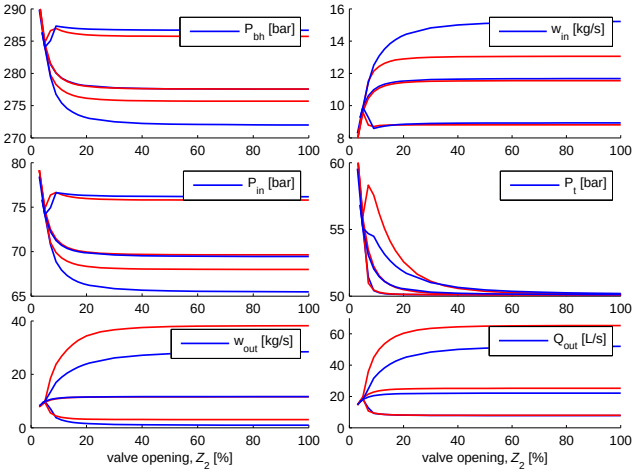

Fig. 2. Bifurcation diagrams of the simplified model (blue) compared to OLGA reference model (red)

The subsea choke valve is considered as flow condition from the well to the pipeline.

$$w_{in} = K_1 z_1 \sqrt{\rho_{mix,t} \max(P_{wh} - P_{in}, 0)}, \tag{17}$$

where P_{in} is pressure at inlet of pipeline which is given by the pipeline-riser model (Jahanshahi and Skogestad (2011)). Flow rates of gas and liquid phases into the pipeline are respectively

$$w_{G,in} = w_{in}\alpha_{G,t}^m + d_1, \tag{18}$$

$$w_{L,in} = w_{in}(1 - \alpha_{G,t}^m) + d_2, \tag{19}$$

where d_1 and d_2 can be assumed as disturbances from the other oil wells in the network.

2.4 Well-pipeline-riser case study

As illustrated in Fig. 1, an oil well was connected to the inlet of the pipeline. The oil well is vertical with depth of 3000 m, the same inner diameter as the pipeline, and the reservoir pressure of 230 bar. Six tuning parameters in the simple model were used for model fitting. The resulting bifurcation diagrams of the simple model are compared to the OLGA reference model in Fig. 2.

3. CONTROLLABILITY ANALYSIS: THEORETICAL BACKGROUND

The state controllability is not our interest in this work; instead the concept of input-output controllability as defined by Skogestad and Postlethwaite (2005) is used.

Definition 1. **(Input-output) controllability** *is the ability to achieve acceptable control performance; that is, to keep outputs (y) within specified bounds or displacement from their references (r), in spite of unknown but bounded variations, such as disturbances (d) and plant changes (including uncertainty), using available inputs (u) and available measurements (y_m and d_m).*

The controllability of the system can be evaluated quantitatively by calculating minimum achievable peaks of different closes-loop transfer functions. These values show the physical limitations of a system in terms of controllability which are dependant on location of poles and zeros of the open-loop system.

3.1 Transfer functions

We assume a linear model in the form $y = G(s)u + G_d(s)d$ with a feedback controller $u = K(s)(r - y - n)$ in which d represents disturbances and n is the measurement noise. The resulting closed-loop system is

$$y = Tr + SG_d d - Tn, \tag{20}$$

where $S = (I + GK)^{-1}$ and $T = GK(I + GK)^{-1} = I - S$ represent the sensitivity and the complementary sensitivity transfer functions, respectively. The control input to the closed-loop plant is

$$u = KS(r - G_d d - n). \tag{21}$$

Moreover, the transfer function SG is related to the effect of input disturbances on the control error $r - y$. One should notice that the closed-loop transfer functions S, T, KS and SG can also be regarded as the measures of robustness against different types of uncertainty. We prefer to keep them as small as possible to achieve better robustness properties of the control system. For instance, the sensitivity transfer function S is also the sensitivity to inverse relative uncertainty, which is a good indication of uncertainty in the pole locations (Skogestad and Postlethwaite (2005)). Therefore, the lowest achievable peaks of the closed-loop transfer functions S, T, KS, SG, KSG_d and SG_d provide information regarding both achievable performance and possible robustness issues.

By the "peak" we mean maximum value of frequency response or $\mathcal{H}_\infty$ norm, $\|M\|_\infty = \max_\omega \|M(j\omega)\|$, which is simply the peak value of the transfer function. The bounds presented in the following are not dependent on the controller K, and they are physical properties of the system itself. The bounds are, however, dependent on a systematic and correct scaling of the system. We will explain scaling of the system later in this Section.

3.2 Lower bound on S and T

The lowest achievable values for peaks of the sensitivity and the complementary sensitivity transfer functions, $M_{S,min}$ and $M_{T,min}$, are calculated based on the distance between the unstable poles (p_i) and zeros (z_i) of the system. For SISO systems, Skogestad and Postlethwaite (2005) give a bound for any unstable (RHP) zero z as the following:

$$\|S\|_\infty \geq M_{S,min} = \prod_{i=1}^{N_p} \frac{|z+p_i|}{|z-p_i|}. \quad (22)$$

The bound increases rapidly as z gets close to p_i, also the bound is tight for a plant with only one RHP-zero. Chen (2000) shows that the bound in equation (22) also applies to $\|T\|_\infty$, and gives the following bound for MIMO systems which is tight for any number of RHP-poles and RHP-zeros:

$$M_{S,min} = M_{T,min} = \sqrt{1+\overline{\sigma}^2(Q_p^{-1/2}Q_{zp}Q_z^{-1/2})}, \quad (23)$$

where the elements of the matrices Q_z, Q_p and Q_{zp} are given by Chen (2000) as

$$[Q_z]_{ij} = \frac{y_{z,i}^H y_{z,j}}{z_i+\overline{z}_j}, [Q_p]_{ij} = \frac{y_{p,i}^H y_{p,j}}{\overline{p}_i+p_j}, [Q_{zp}]_{ij} = \frac{y_{z,i}^H y_{p,j}}{z_i-p_j} \quad (24)$$

The vectors $y_{z,i}$ and $y_{p,i}$ are the (unit) output direction vectors of the zero z_i and pole p_i. Time delay introduces additional limitations; the bounds for $\|T\|_\infty$ is increased by a factor $|e^{p\theta}|$ for a system with single RHP-pole.

3.3 Lower bound on KS

The transfer function KS is from the measurement noise n to the plant input u which is desired to be kept small. The lowest achievable peak for this transfer function can be calculated from the bound (Havre and Skogestad (1997); Havre and Skogestad (2001))

$$\|KS\|_\infty \geq |G_s(p)^{-1}|, \quad (25)$$

where G_s is the stable version of G with the RHP-poles of G mirrored into the LHP. The bound is tight (with equality) for one real unstable pole p. For multiple and complex unstable poles p_i, Glover (1986) derived the tight bound on the transfer function KS

$$\|KS\|_\infty \geq 1/\underline{\sigma}_H(\mathcal{U}(G)^*), \quad (26)$$

where $\underline{\sigma}_H$ is the smallest Hankel singular value and $\mathcal{U}(G)^*$ is the mirror image of the antistable part of G (for a stable plant there is no lower bound).

3.4 Lower bound on SG and SG_d

The transfer function SG is required to be small to reduce the effect of input disturbances on the control error signal, and also for robustness against pole uncertainty. SG_d is related to the effect of disturbances on the outputs. The two following bounds are for any unstable zero z in G (Skogestad and Postlethwaite (2005)):

$$\|SG\|_\infty \geq |G_{ms}(z)| \prod_{i=1}^{N_p} \frac{|z+p_i|}{|z-p_i|}, \quad (27)$$

$$\|SG_d\|_\infty \geq |G_{d,ms}(z)| \prod_{i=1}^{N_p} \frac{|z+p_i|}{|z-p_i|}, \quad (28)$$

where G_{ms} and $G_{d,ms}$ are "minimum-phase, stable version" of the transfer functions G and G_d, respectively (both RHP-poles and RHP-zeros mirrored into LHP). These bounds are only tight for one unstable zeros z, but since they are valid for any RHP-zero z, they can also be used for systems with multiple unstable zeros (Storkaas and Skogestad (2007)).

3.5 Lower bound on KSG_d

In order to calculate the lowest achievable peak for the transfer function KSG_d, the bound in equation (26) can be generalized as (Skogestad and Postlethwaite (2005))

$$\|KSG_d\|_\infty \geq 1/\underline{\sigma}_H(\mathcal{U}(G_{d,ms}^{-1}G)^*). \quad (29)$$

where $\mathcal{U}(G_{d,ms}^{-1}G)^*$ is the mirror image of the anti-stable part of $G_{d,ms}^{-1}G$. This bound is tight for multiple and complex unstable poles p_i. Note that any unstable modes in G_d must be contained in G such that they are stabilizable with feedback control. One simpler approach is to consider the stable, minimum phase part $G_{d,ms}$ of G_d as a weight on KS. Thus, using equation (25) for any unstable pole p (Havre and Skogestad (1997); Skogestad and Postlethwaite (2005)):

$$\|KSG_d\|_\infty = |G_s^{-1}(p)|.|G_{d,ms}(p)|. \quad (30)$$

This bound is only tight for SISO systems with one real unstable pole p.

3.6 Pole vectors

The output pole vector $y_{p,i}$ for a process with state-space representation (A, B, C, D) is defined by (Havre and Skogestad (2003))

$$y_{p,i} = Ct_i, \quad (31)$$

where t_i is the right (normalized) eigenvector associated with p_i ($At_i = p_i t_i$). Based on minimum input usage for stabilization, it can be suggested that the measurements with the largest element in the output pole vector should be used for stabilizing control. In the same way, for input selection, the input that has the largest element in the input pole vector $u_{p,i} = B^H q_i$, where q_i is the left eigenvector of $A(q_i^H A = p_i q_i^H)$ should be used. One limitation on the use of pole vectors is that the relationship between the magnitude of the input usage and the magnitude of the pole vectors elements only hold for a plant with a single unstable pole p. In our system, there is a pair of complex conjugate unstable poles p_i, but pole vectors still give useful information about the measurement selection (Storkaas and Skogestad (2007)).

3.7 Mixed sensitivity controllability analysis

The above controllability measures were also considered by Sivertsen et al. (2009), Storkaas and Skogestad (2007). However, these measures considering only one of transfer

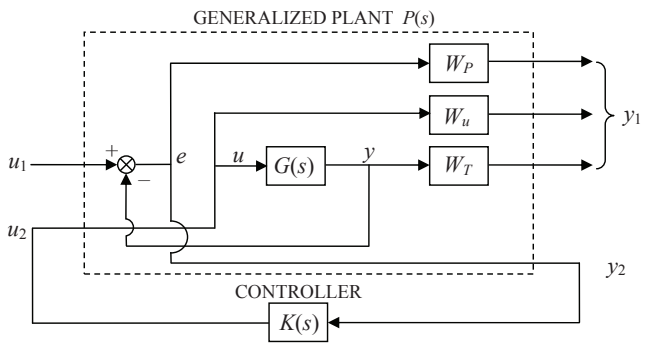

Fig. 3. Closed-loop transfer function for mixed sensitivity control design

functions at any time, may give conflicting results. To get a single measure (γ), we consider an $\mathcal{H}_\infty$ problem where we want to bound $\overline{\sigma}(S)$ for performance, $\overline{\sigma}(T)$ for robustness and to avoid sensitivity to noise and $\overline{\sigma}(KS)$ to penalize large inputs. These requirements may be combined into a stacked $\mathcal{H}_\infty$ problem (Skogestad and Postlethwaite (2005)).

$$\min_K \|N(K)\|_\infty, \quad N \triangleq \begin{bmatrix} W_u KS \\ W_T T \\ W_P S \end{bmatrix} \tag{32}$$

where W_P and W_T determine the desired shapes of sensitivity S and complementary sensitivity T. Typically, W_P^{-1} is chosen to be small at low frequencies to achieve good disturbance attenuation (i.e., performance), and W_T^{-1} is chosen to be small outside the control bandwidth, which helps to ensure good stability margin (i.e., robustness). Solution to this optimization problem is a stabilizing controller K corresponding to S, T and KS which satisfy the following loop shaping inequalities (Glover and Doyle (1988), Doyle et al. (1989)):

$$\begin{aligned} \overline{\sigma}(KS(j\omega)) &\leq \gamma \underline{\sigma}(W_u^{-1}(j\omega)) \\ \overline{\sigma}(T(j\omega)) &\leq \gamma \underline{\sigma}(W_T^{-1}(j\omega)) \\ \overline{\sigma}(S(j\omega)) &\leq \gamma \underline{\sigma}(W_P^{-1}(j\omega)) \end{aligned} \tag{33}$$

To have the same cost function in all simulation tests for the measurement selection, all the candidate control variables shown in Fig. 1 are included in the y_1 port and the control variable(s) for test is in the port y_2 of the generalized plant in Fig. 3. The value of γ in equation (33) should be as small as possible for good controllability.

3.8 Low frequency performance

Disturbance rejection is not the main objective for stabilizing control, but to avoid the possible destabilizing effect of nonlinearity, the system should not "drift" away from its nominal operating point. To achieve low-frequency performance, the steady-state gain of the plant must be large enough. For disturbance rejection and avoiding input saturation, we need $|G(j\omega)| \geq |G_d(j\omega)|$ at the frequencies where $|G_d| > 1$.

3.9 Scaling

One important step before controllability analysis is scaling of inputs, outputs and disturbances of the system. In *Definition 1*, the bound that the control variable must be kept within is not the same for different control variables shown in Fig. 1. For a correct comparison between candidate control variables, they must be scaled based on their maximum allowed variations, in a way that maximum allowed variation for all of them in the scaled model will be (-1,1). The scaling factors D_y for different measurements are given in Table 1 and Table 3. Disturbances in the scaled model are also expected to vary in the range of $(-1, 1)$. The maximum expected values of disturbances (inflow rates) are close to 10% around nominal values of $w_{G,in}$ and $w_{L,in}$. The following values are used for scaling in the both case studies.

$$D_d = \begin{bmatrix} 1 & 0 \\ 0 & 0.04 \end{bmatrix}$$

Controllability analysis is performed at two operating points ($Z_2 = 10\%$ and $Z_2 = 20\%$); therefore the maximum possible changes of u at the two operating points are $D_u = 0.1$ and $D_u = 0.2$ respectively.

4. CONTROLLABILITY ANALYSIS RESULTS

4.1 Pipeline-riser case

Minimum achievable peaks for different closed-loop transfer functions explained in Section 3 are given in Table 1 and Table 2, for two operating points $Z_2 = 10\%$ and $Z_2 = 20\%$ reseptively. Minimum peaks of $|S| = |T|$ for P_t, ρ_m and $\alpha_{L,t}$ in Table 1 are larger than 1, and it is expected to have difficulty using these measurements as control variables. Large values for minimum peak of $|S| = |T|$ are because of RHP-zeros in transfer function of these variables.
Location of RHP-poles of the system and RHP-zeros of P_t for different valve openings are shown in Fig. 4. It can be seen that for $Z_2 = 5\%$ system has a pair of complex conjugate poles on the $J\omega$ axis. For ($Z_2 > 5\%$) two poles are in RHP, and the system becomes unstable. For larger valve openings, one RHP-pole and one RHP-zero get very close to each other. Considering equation (22), when RHP-poles and RHP-zeros are close to each other, the peak of the sensitivity transfer function has a large value. Regarding data given in Table 1 and Table 2, the minimum peak for S and T of P_t is much larger for $Z_2 = 20\%$ compared to its value for $Z_2 = 10\%$.

The other RHP-pole of the system moves far away from the $J\omega$ axis as the valve opening increases. The faster unstable dynamic makes the stabilization more difficult. This effect can be seen by comparing $|KS|$ for $Z_2 = 10\%$ and $Z_2 = 20\%$. It is desired to have larger valve opening and consequently higher production rate, but because of physical limitations of the system in terms of controllability, it is not possible to stabilize the system with a large valve opening.

The minimum achievable peaks of $|S| = |T|$ for Q_{out} and w_{out} are 1, and no problem in term of controllability is expected. But looking at $G(0)$, small steady-state gain leads to poor disturbance rejection. As a result, the system might drift away from the operating point controller designed for locally. The controllability data for the combined measurements in Table 1 and Table 2 show that combining one pressure measurement and one flow

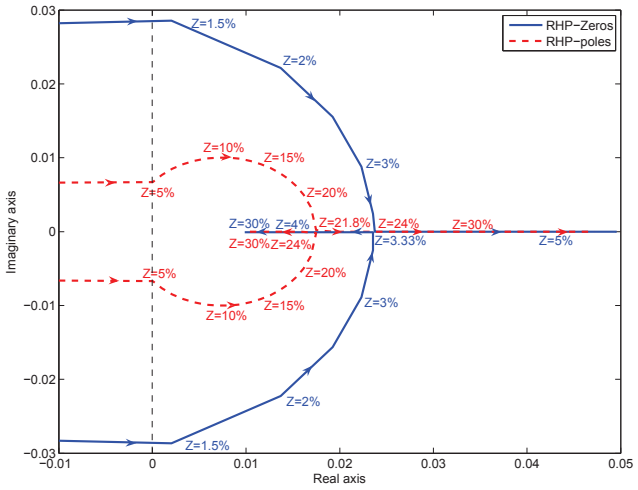

Fig. 4. Location of RHP-poles and RHP-zeros of top pressure of pipeline-riser system for different valve openings

rate gives the best result in terms of controllability. These findings are similar to the results reported by Storkaas and Skogestad (2007) using a two-fluid model. In the next section we extend our analysis to the more general well-pipeline-riser case.

4.2 Well-pipeline-riser case

Controllability data for the two operating points ($Z_2 = 10\%$ and $Z_2 = 20\%$) are given in Table 3 and Table 4. The bottom-hole pressure demonstrates the largest steady-state gain and relatively small values for minimum achievable peaks of all close-loop transfer functions. This means that the pressure at the bottom-hole is an effective control variable. Unlike the pipeline-riser system, Q_{out} and w_{out} show considerable steady-state gains which is result of the pressure-driven nature on the inflows. Therefore, flow rates also can be used in single loop for the stabilizing control without drift problem. Fig. 5 demonstrates the simulation result of $\mathcal{H}_\infty$ control using Q_{out} as the control variable. Considering controllability data for the combined measurements in in Table 3 and Table 4, again combining pressure and flow rate improves the controllability of the system. Simulation result of the $\mathcal{H}_\infty$ control using P_{bh} and Q_{out} as the control variables is illustrated in Fig. 6.

4.3 Mixed Sensitivity Controllability Analysis

The γ values are given in the last column of Table 1, Table 2, Table 3 and Table 4. The control variables with small values of γ are able to control the system with better performance and robustness, also less input usage. The combination of one upstream pressure and the outlet flow results in the smallest value for γ for the two systems.

In some cases, the resulted closed-loop system was unstable. Therefore, calculated γ is considered irrelevant and **'U'** is shown instead of the number. In addition, some control variables under test were not able to minimize the cost function and optimization did not converge; they can be interpreted as ineffective control variables which is in agreement with other controllability data.

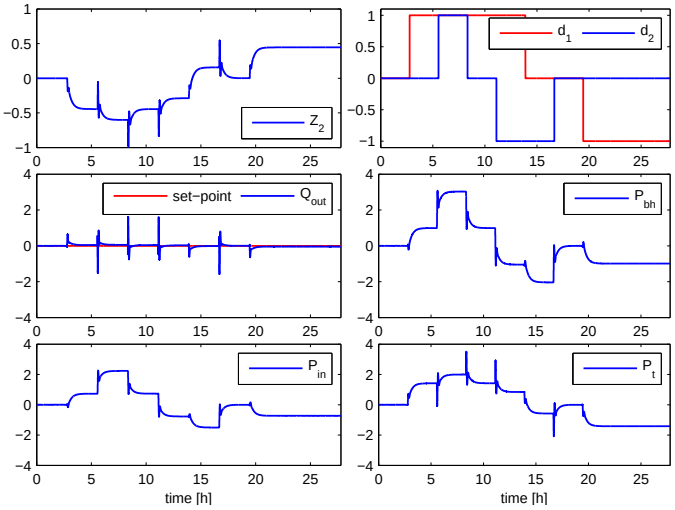

Fig. 5. Result of $\mathcal{H}_\infty$ control using Q_{out} as control variable for well-pipeline-riser system, $Z_2 = 10\%$

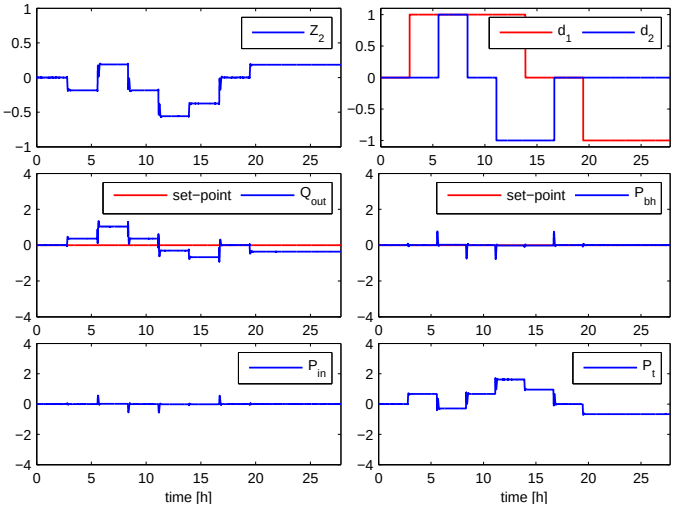

Fig. 6. Result of $\mathcal{H}_\infty$ control using P_{bh} and Q_{out} as control variables for well-pipeline-riser system, $Z_2 = 10\%$

In the $\mathcal{H}_\infty$-analysis, it was observed that for combing one flow rate and one pressure, it is impossible to have tight control on the both at the same time. If tight pressure control is required, flow rate can not be controlled tightly. Because when an inflow disturbance comes to the system, it needs to be released to maintain a constant pressure. In this situation, the flow control can only help for robustness of the pressure control. Simulation result of this case which was used for finding γ value for the well-pipeline-riser case in Table 3 ($Z = 10\%$) is shown in Fig. 7. This desired performance requirement was simulated by considering integral action (i.e. small value for W_P^{-1} at low frequency) for control of P_t and no integral action for Q_{out} (i.e. the weight of $W_P^{-1} = 1/M_s$ in which M_s is the desired peak of sensitivity transfer function). Cascade control with the flow control as the inner loop is a simple structure to implement this case in practice. On the other hand, if tight control on the flow rate is required, the pressure fluctuations because of disturbances are unavoidable.

Table 1. Controllability data for pipeline-riser case study at operating point $Z_2 = 10\%$

Measurement	Value	D_y	$G(0)$	Pole vector	$\|S\| = \|T\|$	$\|KS\|$	$\|SG\|$	$\|KSG_{d1}\|$	$\|KSG_{d2}\|$	$\|SG_{d1}\|$	$\|SG_{d2}\|$	γ
$P_{in}[bar]$	70.28	1	-2.75	0.0065	1	0.67	0	0.21	0.55	0	0	18.91
$P_{rb}[bar]$	68.45	1	-2.76	0.0073	1	0.70	0	0.20	0.64	0	0	15.38
$DP_r[bar]$	17.05	1	-0.20	0.0092	1	0.47	0	0.15	0.55	0	0	82.00
$P_t[bar]$	51.39	1	-2.56	0.0032	3.55	1.34	3.93	0.15	0.73	0.16	0.76	42.30
$Q_{out}[L/s]$	17.94	2	0.19	0.0113	1	0.38	0	0.15	0.67	0	0	83.65
$w_{out}[kg/s]$	9	1	0	0.0118	1	0.37	0	0.15	0.79	0.04	1	100
$\rho_m[kg/m^3]$	501.81	50	-0.21	0.0062	2.94	0.70	5.64	0.26	0.95	0.48	0.13	80.65
$\alpha_{L,t}[-]$	0.58	1	-0.01	0.0004	2.94	11.05	0.34	0.26	0.95	0.03	0.33	–
$P_{in}\&P_t$	–	–	–	–	1	0.6	0	0.21	0.76	0	0	14.93
$P_{in}\&Q_{out}$	–	–	–	–	1	0.33	0	0.20	0.14	0	0	10.37
$P_t\&Q_{out}$	–	–	–	–	1	0.37	0	0.19	0.08	0	0	12.19
$P_t\&\rho_m$	–	–	–	–	1	0.62	0	0.17	0.84	0	0	18.62

Table 2. Controllability data for pipeline-riser case study at operating point $Z_2 = 20\%$

Measurement	Value	D_y	$G(0)$	Pole vector	$\|S\| = \|T\|$	$\|KS\|$	$\|SG\|$	$\|KSG_{d1}\|$	$\|KSG_{d2}\|$	$\|SG_{d1}\|$	$\|SG_{d2}\|$	γ
$P_{in}[bar]$	69.23	1	-0.70	0.0061	1	5.15	0	0.94	2.34	0	0	103.5
$P_{rb}[bar]$	67.40	1	-0.70	0.0081	1	3.91	0	0.83	2.63	0	0	63.13
$DP_r[bar]$	16.97	1	-0.05	0.0092	1	3.41	0	0.66	2.34	0	0	98.35
$P_t[bar]$	50.43	1	-0.65	0.0012	14.25	25.54	2.12	0.65	3.40	0.08	0.40	U
$Q_{out}[L/s]$	18.08	2	0.05	0.0164	1	1.92	0	0.65	3.05	0	0	98.49
$w_{out}[kg/s]$	9	1	0	0.0177	1	1.78	0	0.65	3.80	0.04	1	100
$\rho_m[kg/m^3]$	497.78	50	-0.054	0.0025	32.71	12.45	5.54	3.69	13.30	1.77	0.37	–
$\alpha_{L,t}[-]$	0.57	1	-0.003	0.0002	32.80	196.07	0.35	3.70	13.32	0.11	0.35	–
$P_{in}\&P_t$	–	–	–	–	1	5.05	0	0.68	2.45	0	0	98.98
$P_{in}\&Q_{out}$	–	–	–	–	1	1.80	0	0.68	2.3	0	0	37.45
$P_t\&Q_{out}$	–	–	–	–	1	1.91	0	0.55	2.76	0	0	41.58
$P_t\&\rho_m$	–	–	–	–	1	11.19	0	1.74	6.69	0	0	337.2

Table 3. Controllability data for well-pipeline-riser case study at operating point $Z_2 = 10\%$

Measurement	Value	D_y	$G(0)$	Pole Vector	$\|S\| = \|T\|$	$\|KS\|$	$\|SG\|$	$\|KSG_{d1}\|$	$\|KSG_{d2}\|$	$\|SG_{d1}\|$	$\|SG_{d2}\|$	γ
$P_{bh}[bar]$	281.95	1	-3.80	0.0065	1	0.62	0	0.24	0.46	0	0	20.70
$P_{wh}[bar]$	68.85	1	-2.76	0.0048	1	0.86	0	0.24	0.46	0	0	28.23
$w_{in}[kg/s]$	10.46	1	1.05	0.0037	1	1.10	0	0.24	0.46	0	0	31.02
$P_{in}[bar]$	68.66	1	-2.80	0.0049	1	0.84	0	0.24	0.46	0	0	27.33
$P_{rb}[bar]$	67.26	1	-3.07	0.0059	1	0.70	0	0.23	0.56	0	0	21.21
$DP_r[bar]$	15.54	1	-0.18	0.0088	1.02	0.47	0.03	0.19	0.46	0.033	0.020	89.07
$P_t[bar]$	51.72	1	-2.89	0.0039	3.17	1.05	5.30	0.17	0.54	0.25	0.66	35.48
$Q_{out}[L/s]$	20.66	2	1.24	0.0115	1	0.36	0	0.24	0.53	0	0	28.35
$w_{out}[kg/s]$	10.46	1	1.05	0.0140	1	0.29	0	0.16	0.57	0	0	31.02
$\rho_m[kg/m^3]$	506.56	50	-0.23	0.0055	3.43	0.74	5.50	0.30	0.84	0.69	1.70	85.47
$\alpha_{L,t}[-]$	0.58	1	-0.013	0.0004	3.43	11.70	0.35	0.30	0.84	0.044	0.10	U
$P_{in}\&P_t$	–	–	–	–	1	0.65	0	0.22	0.57	0	0	16.72
$P_{bh}\&Q_{out}$	–	–	–	–	1	0.29	0	0.07	0.04	0	0	8.93
$P_{in}\&Q_{out}$	–	–	–	–	1	0.33	0	0.22	0.76	0	0	12.07
$P_t\&Q_{out}$	–	–	–	–	1	0.34	0	0.06	0.04	0	0	12.64
$P_t\&\rho_m$	–	–	–	–	1	0.61	0	0.23	0.72	0	0	22.84

5. CONCLUSION

The controllability analysis results of the pipeline-riser system using a simplified model are similar to what has been reported in the previous work by Storkaas and Skogestad (2007) using a two-fluid model. Further, we found that the γ value calculated from the $\mathcal{H}_\infty$-analysis predicts a good single measure to compare the controllability of alternative structures.

For SISO control of the pipeline-riser system, a pressure measurement in pipeline is recommended, and the pressure at the riser base demonstrates better result in controllability analysis using the $\mathcal{H}_\infty$ method. For multivariable control, one pressure measurement from the pipeline combined with choke flow rate gives the best result. However, if the subsea measurement is not available, combining top pressure and flow rate gives satisfactory results. Top pressure together with density is able to stabilize the system in theory, if the flow measurement is not available. The measurements $\alpha_{L,t}$ and ρ_m are identified as ineffective control variables for SISO control

The bottom-hole pressure is the best control variable for SISO control of the well-pipeline-riser system. Because of the pressure driven nature of the flow in this case, the flow measurement shows larger steady-state gain and consequently a better performance, compared to the pipeline-riser case. Therefore, having an accurate measurement of flow rate of the choke valve, it can be used in a SISO control scheme for stabilization. Moreover, combining the flow rate with the bottom-hole pressure improves the performance and the robustness considerably.

Table 4. Controllability data for well-pipeline-riser case study at operating point $Z_2 = 20\%$

Measurement	Value	D_y	$G(0)$	Pole vector	$\lvert S\rvert = \lvert T\rvert$	$\lvert KS\rvert$	$\lvert SG\rvert$	$\lvert KSG_{d1}\rvert$	$\lvert KSG_{d2}\rvert$	$\lvert SG_{d1}\rvert$	$\lvert SG_{d2}\rvert$	γ
$P_{bh}[bar]$	280.25	1	-1.15	0.0045	1	3.06	0	0.58	0.95	0	0	U
$P_{wh}[bar]$	67.69	1	-0.83	0.0033	1	4.24	0	0.58	0.95	0	0	–
$w_{in}[kg/s]$	10.93	1	0.32	0.0044	1	2.69	0	0.58	0.95	0	0	98.3
$P_{in}[bar]$	67.48	1	-0.84	0.0035	1	3.89	0	0.58	0.95	0	0	–
$P_{rb}[bar]$	65.98	1	-0.92	0.0060	1	2.12	0	0.58	0.95	0	0	152.3
$DP_r[bar]$	15.43	1	-0.056	0.0087	1.03	1.35	0.02	0.58	0.95	0.034	0.016	104.0
$P_t[bar]$	50.55	1	-0.87	0.0010	12.30	13.63	7.05	0.56	1.44	0.32	0.82	730.5
$Q_{out}[L/s]$	21.79	2	0.37	0.0122	1	1.07	0	0.58	1.20	0	0	67.30
$w_{out}[kg/s]$	10.93	1	0.32	0.0125	1	1.15	0	0.56	1.73	0	0	72.55
$\rho_m[kg/m^3]$	501.63	50	-0.094	0.0012	14.74	15.23	8.74	5.22	10.69	2.76	6.10	–
$\alpha_{L,t}[-]$	0.58	1	-0.006	0.0000	14.64	238.0	0.55	5.19	10.64	0.17	0.39	–
$P_{in}\&P_t$	–	–	–	–	1	2.53	0	0.93	2.04	0	0	110.7
$P_{bh}\&Q_{out}$	–	–	–	–	1	0.89	0	0.93	1.88	0	0	28.46
$P_{in}\&Q_{out}$	–	–	–	–	1	0.90	0	1.57	3.46	0	0	36.77
$P_t\&Q_{out}$	–	–	–	–	1	0.86	0	0.93	1.88	0	0	39.36
$P_t\&\rho_m$	–	–	–	–	1	0.77	0	2.78	5.00	0	0	–

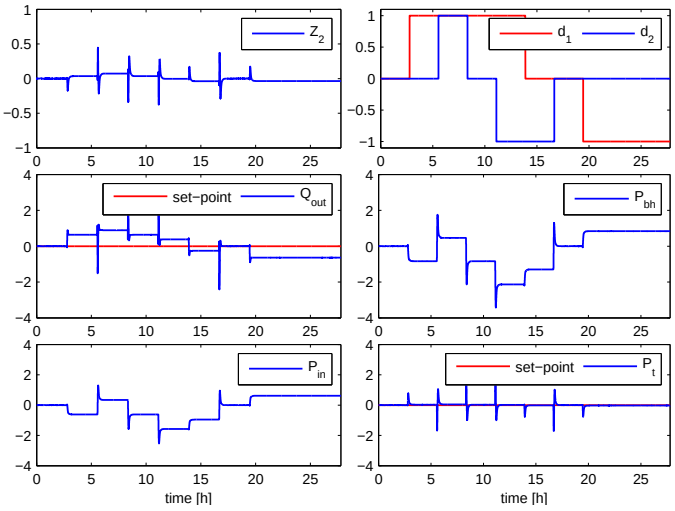

Fig. 7. Result of $\mathcal{H}_\infty$ control using P_t and Q_{out} as control variables for well-pipeline-riser system, $Z_2 = 10\%$

6. FUTURE WORK

The subsea choke valve is a possible manipulated variable, but controllability analysis for only the top-side valve was presented in this paper. A controllability analysis with the subsea choke valve as the manipulated variable, and also the both valves in a MIMO scheme can be beneficial as an extension to this work.

ACKNOWLEDGEMENTS

Financial support for this research was provided by SIEMENS Oil and Gas Division.

REFERENCES

Ahmed, T. (2006). *Reservoir Engineering Handbook, Third Edition*. Elsevier, Oxford, UK.

Chen, J. (2000). Logarithmic integrals, interpolation bounds and performance limitations in mimo feedback systems. *IEEE Transactions on Automatic Control*, 45(6), 1098–1115.

Doyle, J., Glover, K., Khargonekar, P., and Francis, B. (1989). State-space solutions to standard $\mathcal{H}_2$ and $\mathcal{H}_\infty$ control problems. *IEEE Transactions on Automatic Control*, 34(8), 831–847.

Glover, K. (1986). Robust stabilization of linear multivariable systems: relations to approximation. *International Journal of Control*, 43(3), 741–766.

Glover, K. and Doyle, J.C. (1988). State-space formulae for all stabilizing controllers that satisfy an $\mathcal{H}_\infty$-norm bound and relations to relations to risk sensitivity. *Systems and Control Letters*, 11(3), 167–172.

Godhavn, J.M., Fard, M.P., and Fuchs, P.H. (2005). New slug control strategies, tuning rules and experimental results. *Journal of Process Control*, 15, 547557.

Havre, K. and Skogestad, S. (1997). Limitations imposed by rhp zeros/poles in multivariable systems. In *European control conference*. ECC, Brussels.

Havre, K. and Skogestad, S. (2001). Achievable performance of multivariable systems with unstable zeros and poles. *International Journal of Control*, 48, 1131–1139.

Havre, K. and Skogestad, S. (2003). Selection of variables for stabilizing control using pole vectors. *IEEE Transaction on Automatic Control*, 48(8), 1393–1398.

Jahanshahi, E. and Skogestad, S. (2011). Simplified dynamical models for control of severe slugging in multiphase risers. In *18th IFAC World Congress*, 1634–1639. Milan, Italy.

Sivertsen, H., Alstad, V., and Skogestad, S. (2009). Medium-scale experiments on stabilizing riser-slug flow. *SPE Projects, Facilities & Construction*, 4(4), 156–170, SPE no. 120040.

Skofteland, G., Godhavn, J.M., and Kulset, T. (2007). Implementation of a slug control system for subsea wells in an integrated operation environment. In *10th BHR Conference on Multiphase flow*. Edinburgh, UK.

Skogestad, S. and Postlethwaite, I. (2005). *Multivariable Feedback Control: Analysis and Design*. Wiley & Sons, Chichester, West Sussex, UK.

Storkaas, E. (2005). *Stabilizing control and controllability: Control solutions to avoid slug flow in pipeline-riser system*. Ph.D. thesis, Norwegian University of Science and Technology, NTNU.

Storkaas, E. and Skogestad, S. (2007). Controllability analysis of two-phase pipeline-riser systems at riser slugging conditions. *Control Engineering Practice*, 15(5), 567–581.